JOURNAL OF COMPUTATIONAL PHYSICS 85, 323–341 (1989)

Resistive Evolution of Magnetic Fields in Plasmas

G. MILLER, V. FABER, AND A. B. WHITE, JR.

Los Alamos National Laboratory,
Los Alamos, New Mexico 87545

Received July 5, 1988; revised October 24, 1988

In resistive evolution a quasistatic plasma is assumed to be in mechanical equilibrium at every instant of time. Equilibria are determined, in part, by magnetic flux constraints. The evolution of these flux constraints depends only on the electric field parallel to the magnetic field, as given by Ohm's law. The use of a new, magnetic-vector-potential formalism for the resistive evolution problem is discussed. This formalism has advantages of generality and simplicity as well as providing greater numerical accuracy in certain cases (such as the evolution of a magnetic island) where artificial singularities occur when using magnetic surface variables. Sample calculations of the evolution of a strongly driven (pinch) discharge with cylindrical symmetry and of the nonlinear growth of a helically symmetric $m = 2$ magnetic island in the Rutherford regime are given. © 1989 Academic Press, Inc.

I. INTRODUCTION

In many cases the time scale of interest in describing magnetic field behavior in a plasma is much longer than the inertial (Alfvénic) time scale. In such cases it is natural to regard the plasma as satisfying the mechanical equilibrium equations at every instant of time, that is, the quasistatic plasma *evolves* rather than being *dynamic* (see, for example, Refs. [1–3]). Magnetic field evolution in time is governed by the equations

$$-\frac{\partial \mathbf{B}}{\partial t} = \nabla \times \mathbf{E}, \tag{1a}$$

$$\mathbf{E} = -\mathbf{v} \times \mathbf{B} + \eta \mathbf{j}, \tag{1b}$$

$$\mathbf{j} \times \mathbf{B} = \nabla p, \tag{1c}$$

$$\nabla \times \mathbf{B} = \mathbf{j}. \tag{1d}$$

Equations (1a) and (1d) are Maxwell's equations, Eq. (1b) is Ohm's law, and Eq. (1c) is the mechanical equilibrium equation (the equation of motion neglecting the acceleration terms). While Ohm's law in the form given by Eq. (1b) is a

0021-9991/89 $3.00
Copyright © 1989 by Academic Press, Inc.
All rights of reproduction in any form reserved.

simplified approximation, experiment seems to indicate that the component of **E** parallel to **B** is often well represented, and

$$\mathbf{E} \cdot \mathbf{B} = \eta_{\parallel} \mathbf{j} \cdot \mathbf{B}. \tag{2}$$

with $\eta_{\parallel}$ the plasma parallel resistivity, given, for example, in Ref. [4].

Although the velocity **v** appearing in Ohm's law, Eq. (1b), at first sight seems to play a role in the evolution, in fact, magnetic field evolution proceeds independently of **v** and depends only on the component of **E** along **B** given by Eq. (2). This result is obtained by considering, instead of Eq. (1a), the time rate of change of magnetic flux through the circuits formed by a representative set of magnetic field lines [5, 6]. The rate of change of flux is given by

$$-\frac{d}{dt}\oint \mathbf{A} \cdot \mathbf{dl} = -\oint \frac{\partial \mathbf{A}}{\partial t} \cdot \mathbf{dl} = \oint \mathbf{E} \cdot \mathbf{dl}.$$

The fact that **dl** is along **B** means that the rate of change of flux through the circuit is independent of both: (1) components of **E** perpendicular to **B**; and (2) motion of the circuit.

The plasma pressure p and plasma resistivity η also enter into resistive evolution. Additional equations could be written to evolve these quantities, but, for simplicity, p and η are assumed here to be given. In particular, p is here assumed to be zero, since this is a reasonable simplifying assumption for the cases considered.

Equations (1) are thus replaced by

$$-\oint \frac{\partial \mathbf{A}}{\partial t} \cdot \mathbf{dl} = \oint \eta \mathbf{j} \cdot \mathbf{dl}, \tag{3a}$$

$$\mathbf{j} \times \mathbf{B} = 0, \tag{3b}$$

$$\nabla \times \mathbf{B} = \mathbf{j}, \tag{3c}$$

$$\nabla \times \mathbf{A} = \mathbf{B}, \tag{3d}$$

where the line integral in Eq. (3a) is taken along a magnetic field line either until the line closes on itself or "for a very long distance" (a discussion of this is given in Ref. [6]). The determination of electrostatic potential and velocity that, along with the vector potential from Eqs. (3), satisfy Eqs. (1) is discussed, for example, in Ref. [5].

Calculations of resistive evolution of magnetic fields in relatively symmetrical configurations such as the slab, cylinder, or axisymmetric configurations are now commonly done using various formalisms. For 2-dimensional, axisymmetric configurations such as the Tokamak, a formalism using magnetic surface variables is used (see, for example, Refs. [1–3, 7]), and this formalism applies also to compact torus equilibria [8], but not to the more general case of helical symmetry.

Except for the, often very brief, initial phase, where inertia is important, the

growth of magnetic tearing modes is actually resistive evolution [9]. Calculations of such cases have been done in two ways: (1) many authors use the magnetohydrodynamic method, circumventing its inherent difficulties in various ways; or (2) semi-analytic methods, including special orderings, are used (see, for example, Refs. [10–12]).

Taylor's theory of relaxed states [13, 14] provides a prototype for resistive evolution in one special case that has been identified as the limit of a completely ergodic magnetic field [15, 5]. One reason Taylor's method is significant for the present work is its use of the vector potential rather than magnetic surface variables as we shall discuss.

In this paper a new formalism for the resistive evolution problem, closely related to the physical equations in the form given by Eqs. (3), is used. This formalism encompasses the above-mentioned work and is not restricted to axisymmetry. Imperfect magnetic surfaces, and the Taylor limit in particular, can also be treated although the discussion in this paper is limited to the case of perfect magnetic surfaces. A plasma not having magnetic surfaces has many fewer degrees of freedom (the number of representative field lines needed to characterize the plasma) and the computation is therefore much simpler. However, additional physics assumptions (about the broad field-line distribution functions needed) must be made that complicate the discussion.

The new method, like Taylor's, is formulated in terms of the vector potential rather than magnetic surface variables. This has an important advantage of avoiding complicated definitions of toroidal and poloidal fluxes, definitions that are generally different in different flux regions; also, the equations themselves are simpler. Another advantage is that singularities that sometimes occur when using magnetic surface variables, for example, in the case of a magnetic island, are avoided. With a magnetic island, the quantity $\partial\psi/\partial G$ is infinite at the island X point, where ψ is the toroidal magnetic flux and G is the helical flux. The singularity is not physical, in the sense that the magnetic field is certainly not singular (on the contrary, an extremely small change in magnetic field causes the magnetic island). This artificial singularity makes computations using magnetic surface variables less straightforward.

II. Resistive Evolution Equations

The resistive evolution equations, discretized with respect to magnetic field lines, can be written in the form [6]

$$\int -\frac{\partial \mathbf{A}}{\partial t} \cdot \mathbf{B} F_i \, d\tau = \sigma_i \int \eta B^2 F_i \, d\tau, \tag{4a}$$

$$\sigma(\mathbf{r}, t) = \sum_{i=1}^{N} \sigma_i(t) \, F_i[S(\mathbf{r})], \tag{4b}$$

$$F_i \geqslant 0, \tag{4c}$$

$$1 = \sum_{i=1}^{N} F_i, \tag{4d}$$

$$\nabla \times \mathbf{B} = \sigma \mathbf{B}, \tag{4e}$$

$$\nabla \times \mathbf{A} = \mathbf{B}. \tag{4f}$$

B is the magnetic field and **A** the vector potential with the two related by Eq. (4f). The integration in Eq. (4a) is taken over the entire plasma volume with $d\tau$ a volume element. The quantity η is the plasma resistivity, which is assumed for simplicity to be a given spatial function. Crossing Eq. (4e) with **B** we obtain $0 = (\nabla \times \mathbf{B}) \times \mathbf{B}$, which is the plasma mechanical equilibrium equation.

The quantity σ_i is defined by Eqs. (4b), (4c), and (4d). Equation (4b) expresses σ as a sum over N "effective field lines," each having a distribution in space given by F_i with coefficient σ_i. In this paper we consider only the case where the magnetic field forms magnetic surfaces. The distribution function F_i is a function of magnetic surface, labeled by function $S(\mathbf{r})$, so that $F_i = F_i[(S(\mathbf{r})]$. The functions $F_i(S)$ give a measured discretization in the space of magnetic field lines. Each has compact support near a single magnetic surface. The functions $F_i(S)$ need also to satisfy Eqs. (4c) and (4d), and $\{F_i\}$ (the set of all F_i for $i = 1, N$) must spatially characterize the plasma.

In solving Eq. (4f) for **A**, two boundary conditions are needed:

$$\int_{\text{wall}} \mathbf{A} \cdot \mathbf{dl}_{\text{long}} = \chi_{\text{wall}}(t), \tag{5}$$

$$\int_{\text{wall}} \mathbf{A} \cdot \mathbf{dl}_{\text{short}} = \psi_{\text{wall}}(t), \tag{6}$$

where "wall" denotes a toroidal magnetic surface that forms the boundary of the plasma volume (physically this might be a conducting wall with toroidal and poloidal gaps), and the path integrals are taken the long and short way around this toroidal surface. Equation (5) has a different significance than Eq. (6). Equation (5) determines an integration constant in the solution of Eq. (4f) for **A** in terms of **B**, while Eq. (6) constraints the equilibrium equation, determining an integration constant of Eq. (4e), which can be taken as the principal magnetic axis value of the magnetic field, $B_a(t)$.

This system of equations can be conceptually separated into two parts: equilibrium equations that determine **B** and **A** given $\{\sigma_i\}$ and B_a, and time evolution equations allowing $\{\sigma_i(t)\}$ and $B_a(t)$ to be advanced in time. The equilibrium equations consist of the spatially discretized versions of Eqs. (4b) and (4e), with $\{\sigma_i\}$ and B_a as given input parameters. The $N+1$ parameters $\{\sigma_i\}$ and B_a are advanced in time using the $N+1$ equations given by Eq. (4a) for $i = 1, N$ and Eq. (6).

In its computational form, Eq. (4a) calculates $\partial \mathbf{A}/\partial t$ using $(\mathbf{B} - \mathbf{B}^{\text{old}})/\Delta t$, where

$\mathbf{B}^{\text{old}}$, the preceding value of the magnetic field, is the only appearance of a quantity referring to the preceding time value $t = t^{\text{old}}$. All other quantities are evaluated at the current time. Thus, symmetrical time differencing is not used. This scheme is implicit and would be expected to be numerically stable no matter how large the time step Δt. An advantage of nonsymmetrical time differencing is that the limiting case $\Delta t \to \infty$ is meaningful and gives a solution of the steady state problem (Ohmic state).

In the following sections these equations will be discussed and sample calculations presented for the cases of cylindrical and helical symmetry.

III. Cylindrical Symmetry

Cylindrical symmetry means that all quantities depend only on radius r, where r, θ, and z form a cylindrical coordinate system. In component form, Eq. (4e) is then

$$-\frac{\partial B_z}{\partial r} = \sigma B_\theta,$$
$$\frac{1}{r}\frac{\partial}{\partial r}(rB_\theta) = \sigma B_z. \tag{7}$$

These equations are solved on a radial mesh as ordinary differential equations by integrating from $r = 0$ using the initial values $B_\theta(0, t) = 0$, $B_z(0, t) = B_a(t)$.

The functions $F_i(\rho)$ used are shown in Fig. 1 for $N = 10$, where $\rho = r/a$, with a the wall radius ($N = 20$ is used in the cylindrical evolution calculations described below). $F_1(\rho)$ has a small flat region at $\rho = 0$ chosen to have width $1/N$ (as shown in Fig. 1).

The $N + 1$ time evolution equations were solved using a damped Gauss–Newton minimization routine (the sum of the squares of the errors from the $N + 1$ equations

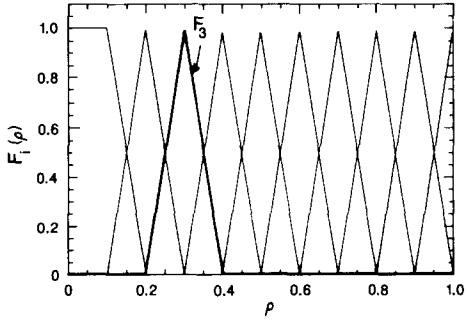

FIG. 1. Field line distribution functions assumed. ρ is a magnetic surface label defined in the text.

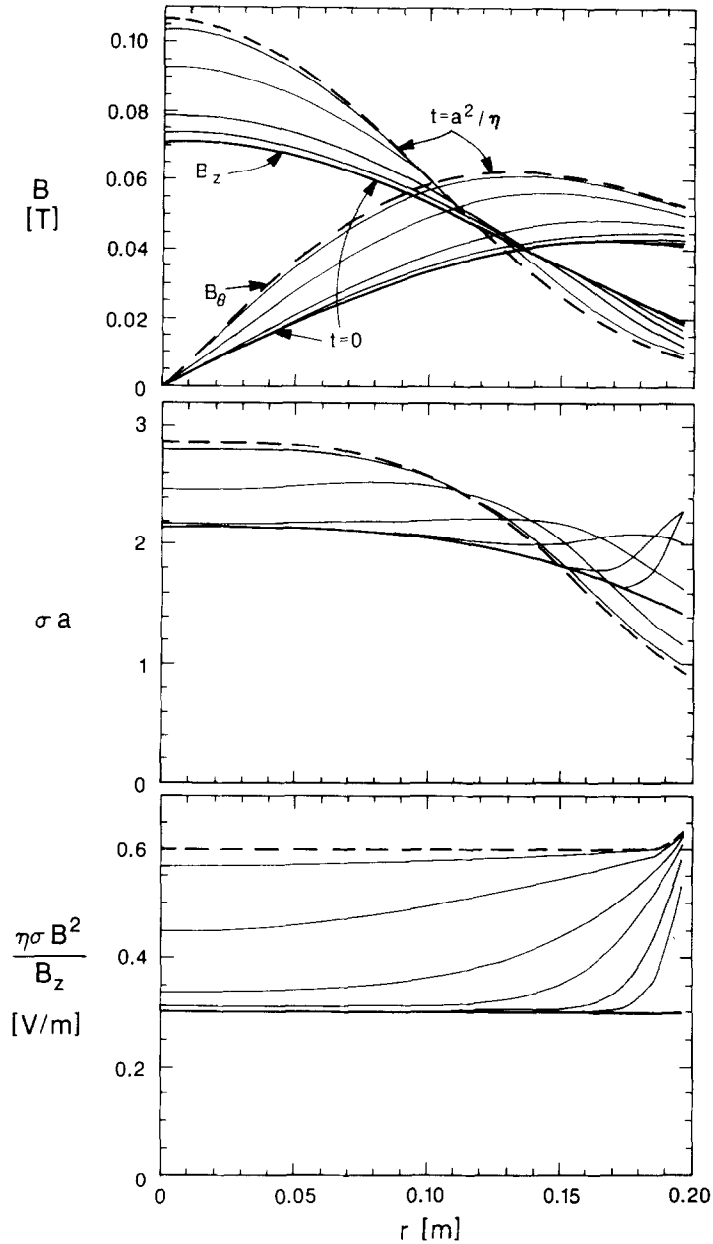

FIG. 2. Evolution of a strongly driven cylindrical discharge in response to a doubling of the driving electric field at $t=0$. Profiles of various magnetic field quantities are shown for the times $t=0.$, 0.001, 0.003, 0.01, 0.03, 0.1, 0.3, and $1.0\,a^2/\eta$.

is minimized) [16]. For one time step, typically only one calculation of the Jacobian was required, followed by a few subsequent iterations without recalculating the Jacobian. For N effective field lines, about $\frac{3}{2}N$ equilibrium calculations are required per time step.

Figure 2 shows a numerical example. The resistivity profile is flat and constant in time. The initial state is a steady (Ohmic) state with applied electric field E and flux ψ such that the dimensionless quantity $Ea^3/(\eta\psi) \simeq 1$, corresponding to a strongly driven discharge. At $t=0$ the electric field is suddenly doubled, with the flux held constant. The graphs show various profiles at times $t=0$, 0.001, 0.01, 0.03, 0.1, 0.3, and $1.0\, a^2/\eta$. A skin effect is apparent in the quantity $E_{\text{res}} = \eta\sigma B^2/B_z$. (In toroidal geometry E_{res} is the resistive toroidal loop voltage divided by the toroidal circumference, $E_{\text{res}} = \int \eta \mathbf{j} \cdot \mathbf{dl}/(2\pi R N_z)$, where the line integral is taken along a magnetic field line.) Figure 2 shows that a time a^2/η well characterizes the time for relaxation to an Ohmic state.

For the results shown in Fig. 2, 20 effective field lines ($N=20$) are used with 41 radial mesh points used in calculating equilibria. Doubling these numbers produced little change in the results.

IV. Helical Symmetry

With helical symmetry, quantities depend on only two variables r and $u \equiv m\theta + kz$, where r, θ, z form a cylindrical coordinate system. Defining

$$G \equiv krA_\theta - mA_z$$

and (8)

$$H \equiv \mathrm{kr}B_\theta - mB_z,$$

with $\mathbf{A}$ the vector potential and $\mathbf{B}$ the magnetic field, one finds [17] from $\mathbf{B} = \nabla \times \mathbf{A}$, $\mathbf{j} = \nabla \times \mathbf{B}$, and $\mathbf{j} \times \mathbf{B} = \nabla p$ that $H = H(G)$, $p = p(G)$, and

$$\frac{\partial^2 G}{\partial r^2} + \frac{1}{r}\frac{m^2 - k^2r^2}{m^2 + k^2r^2}\frac{\partial G}{\partial r} + \frac{m^2 + k^2r^2}{r^2}\frac{\partial^2 G}{\partial u^2}$$

$$= -H\left(\frac{dH}{dG} + \frac{2mk}{m^2 + k^2r^2}\right) - \frac{dp}{dG}(m^2 + k^2r^2). \tag{9}$$

The quantities G and H are magnetic surface quantities (a magnetic surface quantity S satisfies $\mathbf{B} \cdot \nabla S = 0$), in fact,

$$G = \frac{1}{2\pi R}(n\psi - m\chi), \tag{10}$$

and

$$H = \frac{1}{2\pi R}(nI - mJ), \tag{11}$$

where ψ, χ, I, and J are the totoidal and poloidal fluxes of magnetic field and current. The significance of the quantity R is that the helically symmetrical configuration is imagined to be bent into a large-aspect-ratio torus with major radius R, where the only effect of toroidal curvature is to introduce a periodicity constraint into the axial wavenumber k, so that $k = n/R$.

For simplicity, we assume zero pressure in Eq. (9). Then $dH/dG = \sigma(G)$ and equilibria are specified by giving $\sigma(G)$ and the principal magnetic axis value of H, denoted by H_a. Equation (9) can then be solved for $G(r, u)$ [18]. The magnetic fields are given by

$$\begin{aligned} B_r &= -\frac{1}{r}\frac{\partial G}{\partial u} \\ B_\theta &= \frac{1}{m^2 + k^2 r^2}\left(m\frac{\partial G}{\partial r} + krH\right) \\ B_z &= \frac{1}{m^2 + k^2 r^2}\left(kr\frac{\partial G}{\partial r} - mH\right). \end{aligned} \tag{12}$$

To find a vector potential, we choose a gauge with $A_r \equiv 0$. We are free to do this because Eq. (4a) is gauge invariant. The other components of $\mathbf{A}$ are given by

$$A_\theta = \frac{1}{r}\int_0^r r' B_z(r', u)\, dr' \tag{13}$$

$$A_z = A_{za} - \int_0^r B_\theta(r', u)\, dr', \tag{14}$$

where the integration constant A_{za} is the value of A_z at $r = 0$. Boundary conditions involve the gauge invariant fluxes ψ and χ, defined in terms of $\mathbf{A}$ by

$$\psi = \int A_\theta a\, d\theta = a\int_0^{2\pi} A_\theta\, du, \tag{15}$$

$$\chi = \int A_z\, dz = R\int_0^{2\pi} A_z\, du, \tag{16}$$

where both integrals are taken at the wall at $r = a$. By using simple algebra A_{za} can be determined from $\chi(t)$ (or, equivalently, dA_{za}/dt from $d\chi/dt$) using Eqs. (14) and (16).

Resistive evolution with N effective field lines consists in solving the N equations given by Eq. (4a) together with Eq. (15) in the $N+1$ variables σ_i for $i = 1, N$, and H_a.

In resistive evolution of a plasma with helical symmetry, it is convenient to let the magnetic surface label S appearing in the general equations be the helical flux G. As an example we consider the resistive evolution of a configuration with a

magnetic island, as shown in Fig. 3. There are now three different magnetic surface regions: axis—region I, wall—region II, and island—region III.

The field line distributions $F_i(S)$ now must be defined separately in the three regions. We have taken them to be of the simple form shown in Fig. 1, where ρ is now defined as $(G-G_X)/(G_1-G_X)$, with $G_1 = G_a$, G_w, and G_0 in regions I, II, and III, where G_X, G_a, G_w, and G_0 represent the values of G at the X point, axis, wall and 0 point. This rescaling of the flux surface label from G to ρ is trivial as long as G_a, G_0, G_X, and G_w are constants.

A difficulty is that we are specifying equilibria by specifying $\sigma(G)$ and H_a. Thus, the quantities G_a, G_0, G_X, and G_w are results of the equilibrium calculation and are not known beforehand.

In general, G_a, G_0, G_X and G_w can be fixed by varying parameters specifying the solution of Eq. (9), so that at every iteration of Eq. (9), G_a, G_0, G_X, and G_w take given values. Since equilibria are unchanged by adding a constant to G, we need to specify three quantities, say $G_a - G_X$, $G_0 - G_X$, and $G_w - G_X$.

If Eq. (9) is represented by $L(G) = F$, where L is the linear operator appearing on the left-hand side of Eq. (9) and F is the nonlinear functional of G appearing on the right-hand side of Eq. (9), then Newton's step [18] is defined by the linear problem (see Appendix A)

$$L(\delta G) - \frac{\partial F}{\partial G}\delta G = F - L(G) \equiv R. \tag{17}$$

Three additional parameters denoted by α, β, and γ are necessary to keep $G_a - G_X$, $G_0 - G_X$, and $G_w - G_X$ fixed as three additional boundary conditions. The Newton's step then becomes

$$L(\delta G) - \frac{\partial F}{\partial G}\delta G = R + \frac{\partial F}{\partial \alpha}\delta\alpha + \frac{\partial F}{\partial \beta}\partial\beta + \frac{\partial F}{\partial \gamma}\delta\gamma. \tag{18}$$

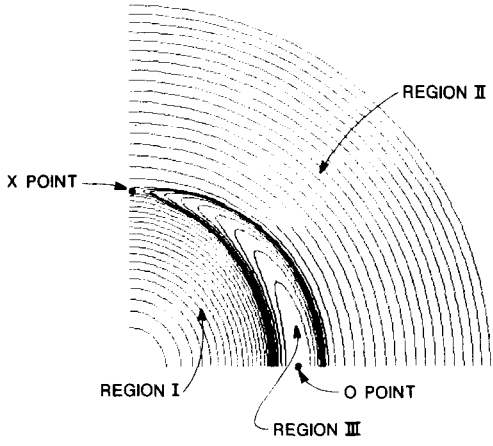

FIG. 3. Helically symmetrical configuration with an $m = 2$ magnetic island. Magnetic surfaces intersecting a plane at constant z are shown.

This is a *linear system of equations in* δG, $\delta\alpha$, $\delta\beta$, and $\delta\gamma$ with three additional boundary conditions determining the three additional variables $\delta\alpha$, $\delta\beta$, and $\delta\gamma$.

We have taken the three additional parameters α, β, and γ to be σ_X, σ_0, and σ_a, where $\sigma(G)$ is represented in the form

$$\sigma = \begin{cases} \sigma_X + (\sigma_a - \sigma_X) f_{\mathrm{I}}(G), & \text{region I,} \\ \sigma_X + (\sigma_w - \sigma_X) f_{\mathrm{II}}(G), & \text{region II,} \\ \sigma_X + (\sigma_0 - \sigma_X) f_{\mathrm{III}}(G), & \text{region III,} \end{cases} \tag{19}$$

with f_{I}, f_{II}, and f_{III} given functions of G varying from 0 at $G = G_X$ to 1 at $G = G_a$, G_0, or G_W. The quantity σ_w, the value of σ at the wall, is an additional parameter.

The enumeration of variables is now as follows. Instead of N variables σ_i for $i = 1, N$, we have the N new variables: $G_a - G_X$; $G_0 - G_X$; $G_w - G_X$; $N-4$ values of $f_k(G)$ for internal field lines in the three regions $k = \mathrm{I}$, II, and III (eliminating the four field lines at the axis, 0 and X points, and wall); and σ_w, the value of σ at the wall.

This scheme allows the domain of functions of G to remain fixed during solution of the equilibrium problem. Note that it is not possible to simply define σ as a function of a scaled flux variable, say ρ as defined above, which varies over the fixed domain $0 \leqslant \rho \leqslant 1$. So defining σ as $\sigma(\rho)$ rather than $\sigma(G)$ leads to an equilibrium problem that is overdetermined.

As an example of a calculation of resistive evolution of a magnetic island we consider the case of the $m = 2$ mode in the Tokamak. The initial configuration is a small island equilibrium obtained by using a 1-dimensional approximation discussed in Appendix A to determine $\sigma(G)$ and to provide and initial guess for the equilibrium solver. The initial 1-dimensional configuration is a cylindrically symmetric steady (Ohmic) state for a particular choice of $\eta(r)$, slightly perturbed by the addition of a small helical field to cause a small magnetic island. In two dimensions, we first find the exact equilibrium corresponding to the 1-dimensional approximation. Then the configuration is allowed to evolve to a new Ohmic state, which is the saturated island state of the $m = 2$ mode. The physics of this process is strongly influenced by the evolution of the resistivity profile. However, being here most interested in methodology, we assume, for simplicity, that $\eta(r)$ is constant in time.

Figure 4 shows a calculation of island growth for a q profile of the form

$$q(r) = C(1 + r^2/r_0^2), \tag{20}$$

as used in Ref. [10], for $r_0 = 0.8$ and C such that the $m = 2$, $n = 1$ rational surface occurs at $r = 0.5$ (assuming $R/a = 3$). Pressure is assumed zero.

Forty effective field lines are used and these define the G contours shown in Fig. 4. Remeshing is done to redistribute the field lines as the island grows. The island grows to most of its full size in about $\Delta t = 0.01\, a^2/\eta(0)$.

The saturated island width (assuming constant $\eta(r)$) is given by $w/a = 0.094$, somewhat smaller than the value 0.13 given in Ref. [10]. The discrepancy might be

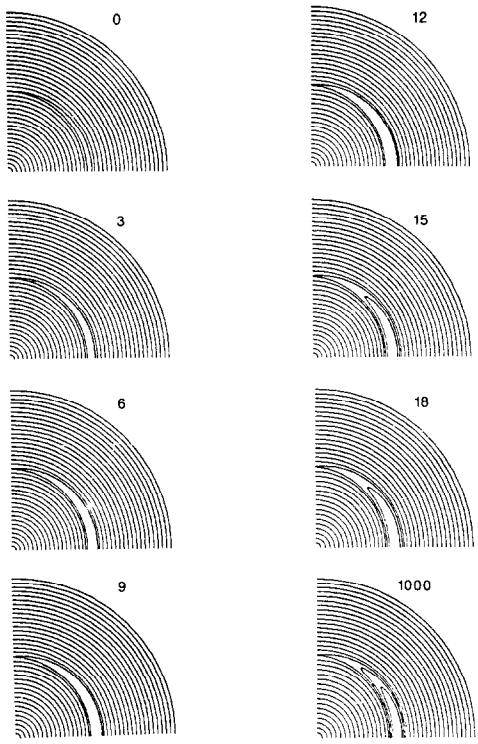

FIG. 4. Magnetic surfaces during growth of an $m=2$ island in a Tokamak. The numbers indicate the elapsed time in units of $0.001\ a^2/\eta(0)$. The calculations assumed 40 effective field lines, and used 216 r mesh points and 14 u mesh points.

accounted for by the use of a quasilinear approximation in Ref. [10]. Figure 5 shows that initial and final σ profiles across the island 0 point. The final σ profile across the island satisfies $\eta_0\sigma_0=\eta_X\sigma_X$ (since $H_0\simeq H_X$, see Appendix B). In the final state $\sigma_0>\sigma_X$ because the radius of the X point is slightly larger than that of the 0 point and thus $\eta_0<\eta_X$.

The nonlinear time evolution equations were solved using the same method discussed in Section III. Solution of the nonlinear equations typically required two calculations of the Jacobian per time step (each calculation of the Jacobian requires $N+2$ equilibrium calculations) plus some number of additional iterations. The fact that the equilibrium calculation itself was iterative and did not have machine precision made the solution of the nonlinear evolution equations more difficult, as the nonlinear solver assumed evaluation with high precision. Also, relative scaling of variables relating to the regions inside and outside of the island was essential for the nonlinear solver to work properly.

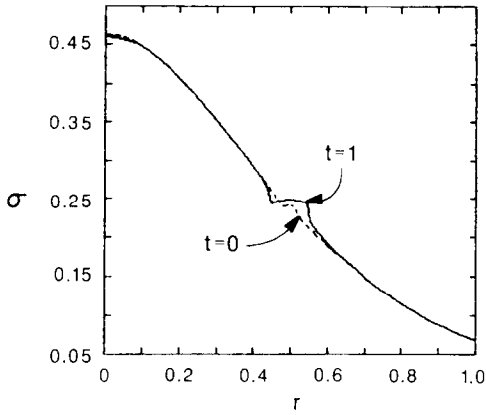

FIG. 5. $\sigma(r)$ profiles through the island 0 point at the initial ($t=0$) and final [$t=a^2/\eta(0)$] times.

V. DISCUSSION

The problem of equilibrium bifurcation is of importance and should be discussed. At a bifurcation point, two distinct equilibrium solutions exist. For example, imagine a cylindrically symmetrical plasma being evolved using the formalism for helical symmetry. A bifurcation point in the evolution occurs when a helically perturbed equilibrium state with $G(r,u)=G_0(r)+G_1(r)\cos(u)$, where G_1 is infinitesimal, becomes possible. That is, Eq. (B2) in Appendix B is satisfied for a $G_1(r)$ that has a continuous derivative as well as satisfying the boundary conditions given by Eqs. (B4) and (B5). At such a bifurcation point the equilibrium solution procedure breaks down and the linear problem defined by Eq. (17) becomes singular. To evolve past a bifurcation point it is usually necessary to jump a finite distance around it, deciding which equilibrium solution branch to follow, e.g., the cylindrically symmetrical one or the helically symmetric one. The proper branch to follow is the most physically relevant one, e.g., the stable branch. Bifurcation points are the points of marginal magnetohydrodynamic stability (where the Euler–Lagrange equation of the energy principle is satisfied). In evolving a cylindrically symmetric configuration, the marginal stability points usually mark the transistion from stability to instability of the cylindrical state toward the helical mode with the given m and k, and not the opposite transistion, since before encountering the bifurcation point the cylindrical state is presumably stable. In this case, at the bifurcation point one should change over to the helical solution.

Broad field line distribution functions F_i are not used for the calculations discussed here. The usefulness of the present formalism is that it allows a unified description of resistive evolution when magnetic surfaces do not exist. In such cases, instead of say 40 effective field lines, two (as used to fit reversed field pinch data [19]) or even one (as in the Taylor ergodic limit) are used, which greatly simplifies the numerical problem. Because such calculations are less computa-

tionally challenging and because of the central importance of additional physics assumptions, these cases are not discussed here. When broad field line distributions are used in situations with cylindrical or helical symmetry, one is implicitly assuming that the magnetic field is weakly stochastic because of three-dimensional effects (a discussion of the possible source of magnetic field stochasticity is given in Ref. [6]), and then consider independently the evolution of the (spatially averaged) underlying configuration with magnetic surfaces.

As 3-dimensional equilibrium calculations become feasible, completely self consistent calculations will be possible, where the F_i's are found by field line tracing of actual calculated magnetic fields at each instant of time without regard for whether or not magnetic surfaces exist.

The computational work in resistive evolution is dominated by the equilibrium calculation. For the 2-dimensional case the computing time for high resolution cases is significant. As discussed in Appendix A, the equilibrium iteration involves solving a large linear system of equations having block tridiagonal structure. Block Gaussian elimination is one method for solving these equations. It is more efficient to ignore the block structure and to consider the linear matrix to be fully banded, making use of optimized band solvers [20]. More efficient still would seem to be the use of multigrid methods [21].

For cylindrical symmetry, including the Shafranov finite aspect ratio corrections if desired (very little extra computing time is necessary for this), resistive evolution using the method discussed here allows very rapid computations.

APPENDIX A: REMARKS ON THE SOLUTION OF THE HELICAL EQUILIBRIUM PROBLEM

The domain of $G(r, u)$ is the region $0 < r < b$ and $0 < u < 2\pi$. As shown in Fig. A1, a conducting wall boundary condition is assumed at $r = b$. The vacuum region from the plasma boundary at $r = a$ to the wall at $r = b$ (if such a region is included) is handled by making use of the Fourier–Bessel function analytic solutions. A vacuum region could, of course, be included in the computational domain, but it is much more efficient to handle such a region separately.

Considered as a function of u alone, $G(u)$ is assumed to have the properties: $G(u)$ periodic over 0, 2π; and $\partial G/\partial u = 0$ at $u = 0$. The boundary conditions at the radial boundaries are expressed in terms of Fourier components, so it is necessary to discuss Fourier transforms. By Fourier's theorem, over the discretized domain $u_j = 2\pi(j-1)/N$, for $j = 1, N$,

$$G(u_j) = \sum_{n=1}^{N} a_n \cos[(n-1)\, u_j]$$
$$a_n = \frac{1}{N} \sum_{j=1}^{N} G(u_j) \cos[(n-1)\, u_j], \tag{A1}$$

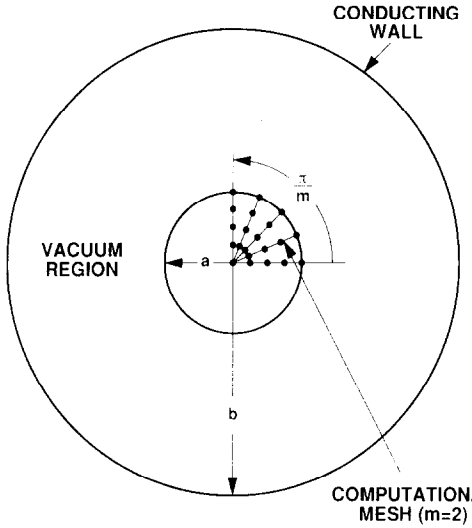

FIG. A1. Geometry of the computational mesh in the r, u plane. Use is made of analytic Fourier–Bessel function solutions in the vacuum region $a < r < b$, if such a region is included.

where a_n is a real mode amplitude. The corresponding sine terms are zero by the requirement that $\partial G/\partial u = 0$ at $u = 0$. The actual computational domain in u consists of only the points $u_j = (j-1)\,\pi/(j_{\max}-1)$ for $j = 1$, $j_{\max}$, where $N = 2(j_{\max}-1)$, using the fact that $G(u_j)$ for $j = 1, N$ is symmetrical about $j = j_{\max}$. This follows from $G(u) = G(2\pi - u)$ (as seen from Eq. (A1)), which also implies that $\partial G/\partial u = 0$ at $u = \pi$. Similarly, the Fourier coefficients a_n are symmetrical about $n = j_{\max}$ so only $j_{\max}$ coefficients need be considered. In terms of the $j_{\max}$ points of the computational domain, Fourier inversion uses the formulae

$$G(u_j) = \sum_{n=1}^{j_{\max}} A_n \cos[(n-1)\,u_j]$$
$$A_n = \frac{2w_n}{j_{\max}-1} \sum_{j=1}^{j_{\max}} w_j G(u_j) \cos[(n-1)\,u_j], \tag{A2}$$

with the weighting w_j defined as: $w_j = 1$ except for $j = 1$ and $j = j_{\max}$ for which $w_j = \frac{1}{2}$.

The boundary conditions on $G(r, u)$ at $r = 0$ and $r = b$ are: $\partial G/\partial r = 0$, $r \to 0$: and $G(b, u) = \text{const}$. The general form of the boundary conditions for $r \to 0$ and $r = a$ is

$$\frac{A_n}{(d/dr)\,A_n} = f_n, \tag{A3}$$

where A_n is the nth Fourier component of $G(u)$ as defined above and f_n is a given quantity. As $r \to 0$, the f_n's are obtained by the requirement of regularity at the

origin with the result that $f_n \to 0$ for $n > 1$ and $f_1 \to \infty$. For $r \to 0$, Eq. (A3) means effectively that the symmetrical Fourier component of G, $A_1(0)$, is a smooth limit of $A_1(r)$ as $r \to 0$. The higher Fourier components, $A_n(0)$ for $n > 1$, are zero.

In the vacuum region, $a < r < b$, Eq. (9) is linear with Bessel function solutions. The quantities f_n, appearing in Eq. (A3), are obtained by demanding continuity from plasma to vacuum of G and $\partial G/\partial r$ at $r = a$ (this is generally not the free boundary condition, see the discussion in Ref. [22]). The answer for $n > 1$, given in Ref. [22], is

$$f_n = \frac{1}{x_2 - 1/x_1}, \tag{A4}$$

where

$$\begin{aligned} x_1 &= \frac{[ka(n-1)]^2}{[m(n-1)]^2 + [ka(n-1)]^2} \frac{K_a'}{K_b'} (I_b' K_a' - I_a' K_b') \\ x_2 &= \frac{[m(n-1)]^2 + [ka(n-1)]^2}{|ka(n-1)|} \frac{K_a}{K_a'}, \end{aligned} \tag{A5}$$

using the simplified Bessel function notation $K_a \equiv K_{m(n-1)}(|ka(n-1)|)$ and so on. For $n = 1$, A_n itself is specified (that is, the average value of G at the wall is specified).

Let i be the discretized variable in the r direction, so that $r_i = (i-1)\, a/(i_{\max} - 1)$. Let δG_i be a vector with $j_{\max}$ components giving $\delta G(r_i, u_j)$ for $j = 1, j_{\max}$. Equation (17) then takes the tridiagonal form

$$A_{i-1} \delta G_{i-1} + B_i \delta G_i + C_i \delta G_{i+1} = R_i + \left(\frac{\partial F}{\partial G}\right)_i \delta G_i, \tag{A6}$$

where δG_i and R_i are column vectors with $j_{\max}$ components and A_i, B_i, C_i, and $(\partial F/\partial G)_i$ are $j_{\max}$ by $j_{\max}$ square matrices given by

$$\begin{aligned} A_i &= \frac{1}{(\Delta r)^2}\left[1 - \frac{m^2 - k^2 r_i^2}{2r_i(m^2 + k^2 r_i^2)} \Delta r\right] I \\ B_i &= -\frac{2}{(\Delta r)^2} I + \frac{m^2 + k^2 r_i^2}{r_i^2 (\Delta u)^2} T \\ C_i &= \frac{1}{(\Delta r)^2}\left[1 + \frac{m^2 - k^2 r_i^2}{2r_i(m^2 + k^2 r_i^2)} \Delta r\right] I, \end{aligned} \tag{A7}$$

where I is the $j_{\max}$ by $j_{\max}$ identity matrix. T is given by

$$T = \begin{bmatrix} -2 & 2 & & & \\ 1 & -2 & 1 & & \\ & 1 & -2 & 1 & \\ & & \cdots & & \\ & & & -2 & 2 \end{bmatrix}. \tag{A8}$$

$(\partial F/\partial G)_i$ is a diagonal $j_{\max}$ by $j_{\max}$ matrix having as its jth diagonal component $\partial F/\partial G(r_i, u_j)$.

Boundary conditions of the general form given by Eq. (A3) result, when discretized, in the equations

$$\begin{aligned} \delta G_1 &= a\,\delta G_2 + b\,\delta G_3 + c \\ \delta G_{i_{\max}} &= x\,\delta G_{i_{\max}-1} + y\,\delta G_{i_{\max}-2} + z, \end{aligned} \tag{A9}$$

where c and z are vectors and a, b, x, and y are $j_{\max}$ by $j_{\max}$ matrices obtained from Eqs. (A3) and (A4) using the Fourier transform relations given by Eqs. (A2). These equations are used to eliminate δG_1 and $\delta G_{i_{\max}}$ from Eqs. (A5), which then can be solved for $\delta G_2, \ldots, \delta G_{i_{\max}-1}$ in terms of $R_2, \ldots, R_{i_{\max}-1}$.

The internal boundary conditions involve the values of G at the magnetic axis, 0 and X points. These points are defined by being roots of the equation $\partial G(r, u_1)/\partial r = 0$, where u_1 is the appropriate value of u (either 0 or π). The evaluation of these internal values of G is discussed in Ref. [18].

Finally, we note that the case $m = 0$ is special in that the value δG_a of δG at the magnetic axis is zero to second order in r as $r \to 0$. Thus, while other cases require variation of three additional parameters α, β, and γ to keep the three quantities $G_a - G_X$, $G_0 - G_X$, and $G_w - G_X$ fixed as discussed in Section IV, for $m = 0$, $G_a - G_X$ is automatically fixed, so variation of only two parameters is required.

APPENDIX B: One-Dimensional Approximation for Small Islands

The analysis given here follows that in Ref. [22] using the present notation. We write $G(r, u)$ in the form

$$G(r, u) = G_0(r) + G_1(r)\cos(u), \tag{B1}$$

where G_1 is small. G_1 approximately satisfies the equation

$$G_1'' + \frac{1}{r}\frac{m^2 - k^2r^2}{m^2 + k^2r^2}G_1' = \left[\frac{m^2 + k^2r^2}{r^2} - \sigma\left(\sigma + \frac{2mk}{m^2 + k^2r^2}\right) - H\frac{d\sigma}{dG}\right]G_1, \tag{B2}$$

where $'$ denotes the radial derivative. Equation (B2) is obtained by substituting Eq. (B1) into Eq. (9) and expanding for G_1 small. H is $H[G_0(r)]$ and σ is $\sigma[G_0(r)]$.

By definition of the island width w, using a formula expressing w in terms of G,

$$G_{1s} \equiv G_1(r_s) = G_0''(r_s)\left(\frac{w}{4}\right)^2, \tag{B3}$$

where r_s denotes the "singular surface" where the island forms. By definition of

r_s, $G_0'(r_s)=0$. Equation (B2) is solved in the regions $(0, r_s)$ and (r_s, a), where a is the wall radius, with boundary conditions

$$G_1 \text{ regular}, r \to 0, \tag{B4}$$

$$G_1(a)=0, \tag{B5}$$

in addition to Eq. (B3). These three boundary conditions imply a discontinuity in the derivative of G_1 at $r=r_s$. The discontinuity in G_1' can be related to discontinuities in B_θ and B_z at r_s, giving the current flowing along field lines in the island region. From Ref. [22],

$$\sigma_0-\sigma_X \simeq -2\frac{[G_1']_s}{wH_s}, \tag{B6}$$

where the square brackets denote the discontinuity in the enclosed quantity, and w is the island width given by Eq. (B3).

This solution identifies $\sigma(G)$ needed as input for the 2-dimensional equilibrium problem. Within the island region, $\sigma(G)$ is linearly interpolated between values at σ_X and σ_0; that is,

$$\sigma(G)=\sigma_X+\frac{G-G_X}{G_0-G_X}(\sigma_0-\sigma_X), \tag{B7}$$

with $\sigma_0-\sigma_X$ from Eq. (B6). Outside the island region $\sigma(G)$ is obtained using the known values of $\sigma_0(r)$ and $G_0(r)$.

$\sigma(G)$ constructed in this way defines a 2-dimensional equilibrium that should closely match the 1-dimensional approximation. Using the 1-dimensional approximation as an initial guess, we find that the 2-dimensional equilibrium solver using Newton's method converges. The agreement between 2-dimensional equilibrium solution and 1-dimensional approximation is quite good for small islands, as shown in Fig. B1. The 1-dimensional approximation allows any size island (the

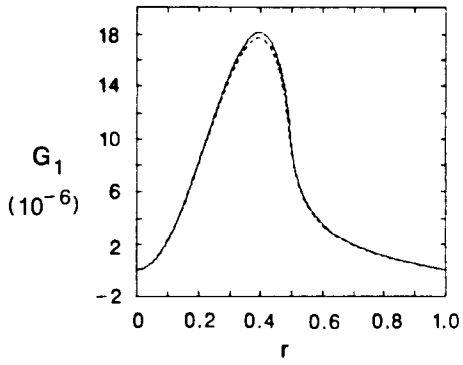

FIG. B1. Exact 2-dimensional equilibrium solution (solid curve) and 1-dimensional approximation (dashed curve) for $G_1(r)$ (the cos(u) Fourier component of $G(r, u)$).

island width w must be specified). The approximation is valid as $w \to 0$. For the case shown in Fig. B1; the 1-dimensional approximation gives the estimate $\sigma_0 - \sigma_X = 0.0052$ from Eq. (B6), while the exact 2-dimensional solution for the same size island gives $\sigma_0 - \sigma_X = 0.0040$.

The resistive evolution of small islands can also be simply treated using the 1-dimensional approximation. Considering field lines at the 0 and X points of the island, Eq. (4a) gives

$$\begin{aligned} \dot{G}_0 &= -\eta_0 H_0 \sigma_0, \\ \dot{G}_X &= -\eta_X H_X \sigma_X, \end{aligned} \tag{B8}$$

where $\dot{}$ denotes a time derivative. Using $G_0 - G_X = 2G_1$, $\eta_X \simeq \eta_0$, and $H_0 \simeq H_X$ and using Eq. (B6), this becomes

$$\dot{G}_1 \simeq \frac{\eta}{w} [G_1']. \tag{B9}$$

Since $w \sim G_1^{1/2}$ from Eq. (B3), Eq. (B9) implies that w grows linearly with time. This approximate equation correctly indicates the initial island growth but does not show island saturation, which can be accurately calculated only by using the exact 2-dimensional evolution equations, including evolution of the resistivity.

REFERENCES

1. H. GRAD, in *Proceedings of the Fourth International Symposium on Computing Methods in Physics, Applied Sciences and Engineering*, edited by R. Glowinski and J. Lions (North-Holland, Amsterdam 1980), p. 261.
2. L. E. ZAKHAROV AND V. D. SHAFRANOV, in *Plasma Physics*, edited by B. Kadomstev (MIR, Moscow, 1981), p. 13.
3. G. V. PEREVERSEV, V. D. SHAFRANOV, AND L. E. ZAKHAROV, in *Theoretical and Computational Plasma Physics* (International Atomic Energy Agency, Vienna, 1978), p. 469.
4. S. I. BRAGINSKII, in *Reviews of Plasma Physics, Vol. I*, edited by M. A. Leontovich (consultants Bureau, New York, 1965), p. 205.
5. G. MILLER, *Phys. Fluids* **28**, 1354 (1985).
6. G. MILLER, *Phys. Fluids* **31**, 1133 (1988).
7. J. HOGAN, *Nucl. Fusion* **19**, 753 (1979).
8. D. E. SHUMAKER, *J. Comput. Phys.* **53**, 456 (1984).
9. P. H. RUTHERFORD, *Phys. Fluids* **16**, 1903 (1973).
10. R. B. WHITE, D. A. MONTICELLO, M. N. ROSENBLUTH, AND B. V. WADDELL, *Phys. Fluids* **20**, 800 (1977).
11. A. SYKES AND J. WESSON, in *Plasma Physics and Controlled Nuclear Fusion Research, 1980, Vol. I* (International Atomic Energy Agency, Vienna, 1981), p. 237.
12. B. V. WADDELL, M. N. ROSENBLUTH, D. A. MONTICELLO, R. B. WHITE, AND B. CARRERAS, in *Theoretical and Computational Plasma Physics, Trieste, March* 1977 (International Atomic Energy Agency, Vienna, 1978).

13. J. B. TAYLOR, *Phys. Rev. Lett.* **23**, 1139 (1974).
14. J. B. TAYLOR, in *Pulsed High Beta Plasmas*, edited by D. Evans (Pergamon, Oxford, 1976), p. 59.
15. G. MILLER, *Phys. Fluids* **28**, 308 (1985).
16. K. KLARE, Program *GN*, Los Alamos National Laboratory, 1986 (unpublished).
17. J. L. JOHNSON, C. R. OBERMAN, R. M. KULSRUD, AND E. A. FRIEMAN, *Phys. Fluids* **1**, 281 (1958).
18. G. MILLER, V. FABER, AND A. B. WHITE, *J. Comput. Phys.* **79**, 417 (1988).
19. G. MILLER, *Phys. Fluids* **31**, 3330 (1988).
20. D. CALAHAN, with revisions by T. JORDAN, program BANSOL, Los Alamos National Laboratory, 1987 (unpublished).
21. W. L. BRIGGS, *A Multigrid Tutorial* (SIAM, Philadelphia, 1987).
22. G. MILLER, *Phys. Fluids* **28**, 560 (1985).